Electronic Supplementary Information for

Aggregation-dependent photovoltaic properties of squaraine/PC61BM bulk heterojunctions

Kaja C. Deing, Ulrich Mayerhöffer, Frank Würthner* and Klaus Meerholz*

K. C. Deing, Prof. Dr. K. Meerholz
Department of Chemistry
Universität zu Köln
Luxemburgerstr. 116, 50939 Köln (Germany)
Fax: (+49)221-470-5144
E-mail: klaus.meerholz@uni-koeln.de

U. Mayerhöffer, Prof. Dr. F. Würthner
Institut für Organische Chemie and Röntgen Research
Center for Complex Material Systems
Universität Würzburg
Am Hubland, 97074 Würzburg (Germany)
E-mail: wuerthner@chemie.uni-wuerzburg.de

Table of Contents

Synthesis and Characterization of Squaraines

Procedure for the synthesis of **3-[(3-Butyl-1,3-benzothiazol-2(3*H*)-ylidene)methyl]-4-ethoxycyclobut-3-ene-1,2-dione:**

A portion of 2.35 g (7.06 mmol) of *N*-butyl-benzothiazolium iodide and 1 mL triethylamine were dissolved in 8 mL ethanol and heated to reflux. Under reflux, 1.00 g (5.88 mmol) 3,4-diethoxy-3-cyclobutene-1,2-dione were added. After 15 min the solution was allowed to cool down and the solvent was evaporated under reduced pressure. The crude products were purified by column chromatography (silica gel, EtOAc).

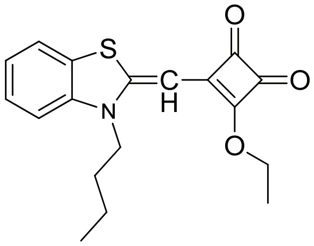

$C_{18}H_{19}NO_3S$ (329.41)
Yield: 3.54 g (10.8 mmol, 92 %), orange solid.
M.p.: 154 °C. ^{1}H NMR (400 MHz, $CDCl_3$, TMS): $\delta = 7.49$ (ddd, $^3J(H,H) = 7.8$ Hz, $^4J(H,H) = 1.2$ Hz, $^5J(H,H) = 0.4$ Hz, 1H, CH_{arom}), 7.33 (td, $^3J(H,H) = 7.5$ Hz, $^4J(H,H) = 1.2$ Hz, 1H, CH_{arom}), 7.16 (td, $^3J(H,H) = 7.5$ Hz, $^4J(H,H) = 1.0$ Hz, 1H, CH_{arom}), 7.06 (d, $^3J(H,H) = 7.8$ Hz, 1H, CH_{arom}), 4.85 (q, $^3J(H,H) = 7.1$ Hz, 2H, O-CH_2), 3.98 (t, $^3J(H,H) = 9.4$ Hz, 2H, N-CH_2), 1.81 (m, 2H, CH_2), 1.53 (t, $^3J(H,H) = 7.1$ Hz, 3H, CH_3), 1.49 (m, 2H, CH_2), 1.02 (t, $^3J(H,H) = 7.3$ Hz, 3H, CH_3). HRMS (ESI, pos. mode, acetonitrile/$CHCl_3$): m/z 329.10801 [M^+] (calcd for $C_{18}H_{19}NO_3S$ 329.10802).

Procedure for the synthesis of **Triethylammonium 2-[(3-butyl-1,3-benzothiazol-2(3*H*)-ylidene)methyl]-3-(dicyanomethylidene)-4-oxocyclobut-1-en-1-olate:**

Triethylamine (0.5 mL) was added dropwise under stirring to a solution of 606 mg (1.84 mmol) of 3-[(3-Butyl-1,3-benzothiazol-2(3*H*)-ylidene)methyl]-4-ethoxycyclobut-3-ene-1,2-dione and 787 mg (1.99 mmol) of malononitrile in 35 mL ethanol. The stirring was continued for additional 2 h at room temperature. Afterwards, the solvent was removed under reduced pressure and the solid residue was purified by column chromatography (silica gel, CH_2Cl_2/MeOH 95:5).

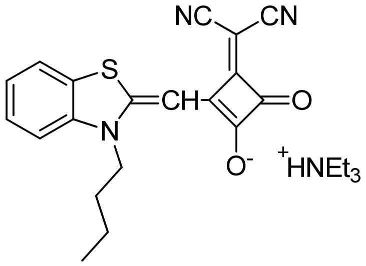

$C_{25}H_{30}N_4O_2S$ (450.59)
Yield: 3.32 g (7.39 mmol, 70 %), orange solid.
M.p.: > 180 °C (decomp.). ^{1}H NMR (400 MHz, $CDCl_3$, TMS): $\delta = 7.44$ (dd, ^3J(H,H) = 7.8 Hz, ^4J(H,H) = 0.8 Hz, 1H, CH_{arom}), 7.22 (t, ^3J(H,H) = 8.4 Hz, 1H, CH_{arom}), 7.07 (d, ^3J(H,H) = 8.1 Hz, 1H, CH_{arom}), 7.04 (t, ^3J(H,H) = 7.8 Hz, 1H, CH_{arom}), 5.81 (s, 1H, $CH_{methylen}$), 3.53 (q, ^3J(H,H) = 7.1 Hz, 2H, N-CH_2), 3.05 (q, ^3J(H,H) = 7.3 Hz, 6H, N^+-CH_2), 1.62 (m, 2H, CH_2), 1.38 (m, 2H, CH_2), 1.17 (t, ^3J(H,H) = 7.3 Hz, 9H, CH_3), 0.89 (t, ^3J(H,H) = 7.3 Hz, 3H, CH_3). HRMS (ESI, neg. mode, acetonitrile/$CHCl_3$): *m*/*z* 348.08121 [M^--($HNEt_3^+$)] (calcd for $C_{19}H_{14}N_3O_2S$ 348.08122).

General procedure for the synthesis of dicyanovinyl-substituted squaraines **S-Se** and **O-S**:
A portion of 603 mg (1.34 mmol) of triethylammonium 2-[(3-butyl-1,3-benzothiazol-2(3*H*)-ylidene)methyl]-3-(dicyanomethylidene)-4-oxocyclobut-1-en-1-olate and 1.37 mmol of the appropriate iodide were heated under reflux in a mixture of 50 mL of a *n*-butanol/benzene mixture (1:1 v/v) for 8 h using a Dean-Stark trap. The solvent was removed under reduced pressure and the residue was purified by column chromatography (silica gel, CH_2Cl_2/MeOH (0-2 %)) to afford the corresponding squaraines **S-Se** and **O-S**.

Squaraine **S-Se**:

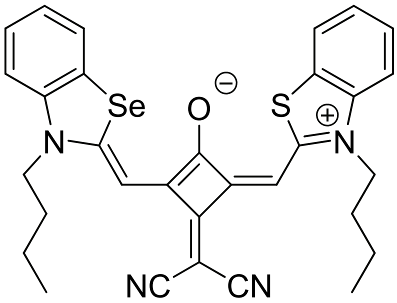

Yield: 448 mg (768 µmol, 32%), blue solid.

mp.: 333°C.

^{1}H NMR (400 MHz, CD_2Cl_2, TMS): $\delta = 7.58$ (m, 2H, CH_{arom}), 7.38 (m, 2H, CH_{arom}), 7.21 (m, 2H, CH_{arom}), 7.13 (m, 2H, CH_{arom}), 6.39 (s, 1H, CH), 6.26 (s, 1H, CH), 4.05 (q, ^3J(H,H) = 8.9, 4H, NCH_2), 1.73 (m, 4H, CH_2), 1.42 (m, 4H, CH_2), 0.93 (dt, ^{3}J(H,H) = 8.4, ^{4}J(H,H) = 1.8, 6H, CH_3).

HRMS (ESI, positiv, Acetonitril / Chloroform): m/z: 578.12026 (M^+) calculated for $C_{31}H_{28}N_4OSSe$: 578.12031.

CHN: calculated for $C_{31}H_{28}N_4OSSe$: C, 63.80; H, 4.84; N, 9.60; S, 5.49. found: C, 63.94; H, 4.84; N, 9.78; S, 5.55.

UV/VIS (DCM; $c = 1\cdot10^{-6}$ M): λ_{max} [nm] (ε [$M^{-1}cm^{-1}$]) = 709 (170000); 380 (36000).

CV (CH_2Cl_2, 0.1 M TBAHFP, Fc/Fc^+): E_{red} (X^-/X) = –1599 mV, E_{ox} (X/X^+) = –8.00 mV, E_{ox} (X^+/X^{2+}) = 507.0 mV.

Squaraine **O-S**:

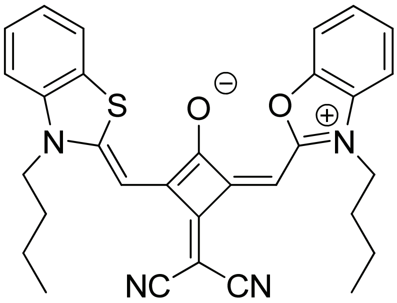

Yield: 364 mg (699 µmol, 16%), blue solid.

mp.: 304°C.

^{1}H NMR (400 MHz, CD_2Cl_2, TMS): δ = 7.59 (d, ^{3}J(H,H) = 7.84, 1H, CH_{arom}), 7.40 (t, ^{4}J(H,H) = 1.24, 1H, CH_{arom}), 7.37 (t, ^{3}J(H,H) = 7.60, 1H, CH_{arom}), 7.28 (t, ^{3}J(H,H) = 7.60, 1H, CH_{arom}), 7.22 (t, ^{3}J(H,H) = 8.64, 3H, CH_{arom}), 7.12 (d, ^{4}J(H,H) = 1.00, 1H, CH_{arom}), 5.66 (s, 1H, CH), 6.28 (s, 1H, CH), 4.07 (t, ^{3}J(H,H) = 7.72, 2H, NCH_2), 3.92 (t, ^{3}J(H,H) = 7.52, 2H, NCH_2), 1.78 (m, 4H, CH_2), 1.41 (m, 4H, CH_2), 0.93 (q, ^{3}J(H,H) = 7.44, 6H, CH_3).

HRMS (ESI, positiv, Acetonitril / Chloroform): m/z: 520.19277 (M^+) calculated for $C_{31}H_{28}N_4O_2S$: 520.19275.

CHN: calculated for $C_{31}H_{28}N_4O_2S$: C, 71.51; H, 5.42; N, 10.76; S, 6.16. found: C, 71.33; H, 5.31; N, 10.88; S, 6.03.

UV/VIS (DCM; $c = 1\cdot10^{-6}$ M): λ_{max} [nm] (ε [$M^{-1}cm^{-1}$]) = 664 (160000); 397 (44000).

CV (CH_2Cl_2, 0.1 M TBAHFP, Fc/Fc^+): E_{red} (X^-/X) = −1710 mV, E_{ox} (X/X^+) = –3.50 mV, E_{ox} (X^+/X^{2+}) = 523.5 mV.

Cyclic Voltammetry

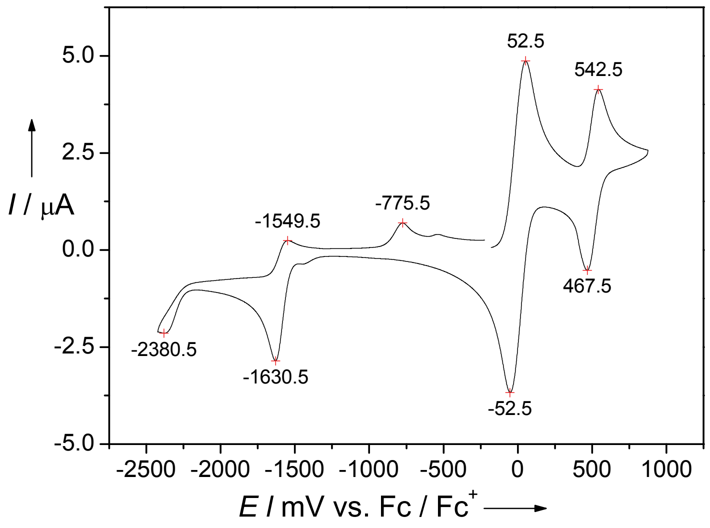

Figure S1. Cyclic voltammogram of squaraine **S-S** in CH_2Cl_2 ($c = 3.6 \times 10^{-4}$ M; calibrated vs. Fc/Fc^+). Scan rate 100 mV s^{-1}; supporting electrolyte TBAHFP (0.1 M).

Table S1. Electronic properties of the investigated squaraine dyes determined by cyclic voltammetry calibrated against the ferrocene/ferrocenium redox couple.[a)]

Dye	$E_{1/2}$(Ox) / V	$E_{1/2}$(Ox) / V	E_p(Red) / V	E_{HOMO} / eV	E_{LUMO} / eV
O-O	0.009	0.536	–1.789	-5.16	-3.36
O-S	–0.0035	0.5235	–1.710	-5.09	-3.44
S-S	–0.013	0.505	–1.630	-5.14	-3.52
S-Se	–0.008	0.507	–1.599	-5.10	-3.55

[a)] for the reversible oxidation processes in cyclic voltammetry measurements half-wave potentials are given (calculated from the average value of the oxidation and reduction peak potentials) whilst for the irreversible reduction processes the peak potentials of the reduction waves are given.

Device Fabrication and Measurements

All solar cell devices were fabricated on commercial indium-tin oxide (ITO) coated glass. The ITO was etched with acid ($HCl/FeCl_3$) and subsequently cleaned with chloroform, acetone, mucasol detergent, and de-ionized water in ultrasonic bath.

The ITO substrates were then exposed to ozone for 10 min and immediately coated with poly(3,4-ethylene dioxythiophene):poly(styrene sulfonate) (PEDOT:PSS) (Baytron P AL 4083, HC Starck; ca. 30 nm). Afterwards, the samples were heat treated for 1 min at 110 °C to remove residual water and transferred into a N_2 glove box for further device fabrication process and measurements.

PCBM was obtained from a commercial supplier (Nano-C, Westwood, USA) and the squaraine dyes were synthesized according to previously described procedures (for compound characterization of O-S and S-Se see below).[a] The active layers were spin-coated from chloroform solutions containing the respective squaraine derivative and PCBM.

A Dektak surface profiler (Veeco) was used to determine the active layer thickness. The active layer thickness ranged between 80 and 90 (± 5) nm. No significant influence of the layer thickness within this range on the device performance has been observed. UV/Vis spectra of these films were taken with a Varian Cary 50 spectrometer.

The substrates were moved to a high-vacuum chamber where the top electrode was evaporated through a mask (6 nm Ca, 120 nm Al), leading to seven solar cells on each substrate with an active area of 0.08 cm^2.

The *J-V* characteristics of the solar cells were measured by using a Keithley 2425 source measurement unit. The AM 1.5 light was provided by a filtered Xe lamp. The intensity of 100 $mW\ cm^{-2}$ of the AM 1.5 light was determined by using a calibrated inorganic solar cell from the Fraunhofer Institute for Solar Research in Freiburg (Germany) and a reference $P3HT/PC_{61}BM$ cell measured by the same institution. No spectral mismatch factor was included in the calculation of the efficiency. *EQE* spectra were measured using color filters from Melles Griot.

Local current mapping was done on a photocurrent tester developed and manufactured in collaboration with Botest Systems GmbH and the Institute of Physical Chemistry in Cologne. The photocurrent was measured locally in short circuit condition illuminated by a laser spotlight of a diameter of 40 μm and a power output of 3 mW at 405 nm wavelength.

---

[a] U. Mayerhöffer, K. Deing, K. Gruss, H. Braunschweig, K. Meerholz and F. Würthner, *Angew. Chem. Int. Ed.* 2009, **48**, 8776.

Absorption spectra were measured with an UV-VIS Spectrophotometer Cary 50 Bio from Varian. In the case of the solar cells that form different domains, the metal electrode was removed with adhesive foil. The substrate was then covered with a shadow mask exposing only the active device area to the measuring laser beam.

The influence of the metal top-layer on aggregation

The importance of the metal coating for aggregation becomes clear by comparing the annealed device after removal of the metal coating and the free film. The photographs in Figure S2 show the **S-S**/PC$_{61}$BM blend after annealing at 110 °C. The area where the electrode has been located is shown on the left side (a). Here a uniform blue color is observed that can be attributed to a homogeneous **R** domain consisting of J-aggregated squaraines. The black spots correspond to possible nucleation centers. Note that most nucleation centers do not necessarily lead to aggregation. The ancient border between the former electrode covered area and the free film is clearly visible (black line) and accompanied by a transition zone (dotted line) before merging into the free film morphology. In the free film (b) one can distinguish four different domain growing schemes (b1-b4). These different islands differ in terms of form, size and texture demonstrating the structural diversity of the **S-S**/PC$_{61}$BM blend. According to the form of growth the blue egg shaped domains (b4) most likely correspond to **R** domain but no definite assignment is possible. Photographs were taken with a Zeiss Axio microscope.

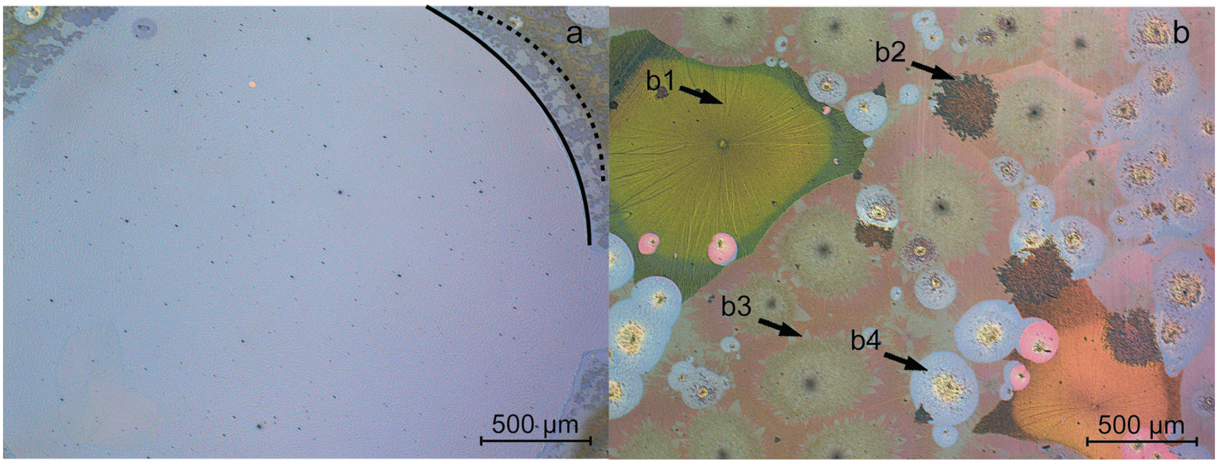

Figure S2. Photographs of the annealed contact of **S-S**/PC$_{61}$BM blend at 110 °C (a) and the free film (b) (no metal top layer during annealing) both located on the same substrate. The donor content of the **S-S**/PC$_{61}$BM blend is 60 % by weight. The metal top layer has been removed prior to microscopic investigation.

Field effect mobility measurements

Transistors were fabricated by spin-coating of chloroform solution of the **S-S**/PC$_{61}$BM blend on pre-fabricated heavily doped p-type Si+/SiO$_X$ substrates with patterned source and drain gold contacts. The doped silicon substrate was used as the gate contact, followed by a 230 nm thick SiO$_X$ insulating layer with a capacitance of 15 nF cm^{-2}. Channel length and width were 10 µm and 1 cm, respectively. Film thickness of the active layers was estimated to be around 60 nm. Devices were measured in a dry nitrogen atmosphere with a Keithley 4200-SCS semiconductor characterization system. Mobilities were calculated from the transconductance in the linear regime. Prior to annealing, a metal top-layer was deposited on the active layer to provide comparable domain formation. The metal top-layer has been ripped off before the measurement. Note that electron mobility could only been measured if annealed at 150 °C with a metal top-layer.

Table S2. Field effect mobility ($\mu_{\text{lin.}}$) of the **S-S**/PC$_{61}$BM blend.

thermal treatment	$\mu_{\text{lin.}}$ / cm^2 V^{-1}s^{-1} h$^+$	$\mu_{\text{lin.}}$ / cm^2 V^{-1}s^{-1} e$^-$
none	3x10^{-6}	-
110°C	3x10^{-5}	-
150°C	2x10^{-5}	4x10^{-4}